J. Membrane Biol. 88, 139–147 (1985)

The Journal of
Membrane Biology

Resistance Properties of the Diluting Segment of *Amphiuma* Kidney: Influence of Potassium Adaptation

Hans Oberleithner*, William Guggino**, and Gerhard Giebisch
Department of Physiology, Yale University School of Medicine, New Haven, Connecticut

Summary. Chronic exposure to high potassium stimulates K^+-secretory mechanisms in the diluting segment of the amphibian kidney (K^+ adaptation). Since K^+ net flux depends critically on the passive cell membrane permeabilities for K^+ ions, cable analysis and K^+-concentration step changes were applied in this nephron segment to assess the individual resistances of the epithelium and the K^+ conductance of the luminal cell membrane. Experiments were performed in the isolated, doubly-perfused kidney of both control and K^+-adapted *Amphiuma*. In control animals transepithelial resistance was 290 ± 27 Ωcm^2, which decreased significantly to 199 ± 17 Ωcm^2 after K^+ adaptation. The resistance in parallel of the luminal and peritubular cell membrane decreased from a control value of 157 ± 14 to 108 ± 6 Ωcm^2 after chronic K^+ treatment. This was paralleled by a decrease of the ratio of the luminal to peritubular cell membrane resistance from 2.5 ± 0.1 to 1.9 ± 0.1, respectively. Estimation of the individual cell membrane resistances reveals that the combined resistance of the luminal and peritubular cell membrane is in the same order of magnitude as the paracellular shunt resistance in diluting segments of both control and K^+-adapted animals. The luminal cell membrane is K^+ selective under both conditions, but the absolute luminal K^+ conductance increases by some 60% with K^+ adaptation. This leads to an increased back-leak of K^+ from cell to lumen and may explain stimulated K^+ net secretion found after chronic K^+ loading.

Key Words diluting segment · K^+ conductance · K^+ adaptation · cable analysis · K^+ transport

Introduction

Similar to the mammalian thick ascending limb [4, 9, 15], the amphibian diluting segment is characterized by a luminal K^+ permeable and a peritubular Cl^- permeable cell membrane [22, 27]. These passive cell membrane properties in conjunction with a secondary active Na^+, Cl^-, K^+ luminal cotransporter, driven by a favorable (lumen-to-cell oriented) Na^+ gradient, allow transcellular net transport of solutes from lumen to blood. Low intracellular Na^+ is maintained by the energy (ATP)-consuming Na^+/K^+ pump located in the peritubular cell membrane [11, 25].

When amphibians are chronically exposed to high potassium (i.e., keeping amphibians in a solution of 50 mmol/liter KCl for at least 3 days), the functional properties of the diluting segment of the kidney are found dramatically altered. After the so-called K^+ adaptation (i) the direction of transepithelial K^+ net flux is reversed from K^+ net reabsorption into K^+ net secretion [21, 34], (ii) transepithelial Cl^- transport is altered [24] and (iii) H^+ net secretion is stimulated [23]. Recent experiments [33] indicate that the corticosteroid hormone aldosterone modulates the transport function of the amphibian diluting segment, a hormone which is found significantly elevated in the plasma of K^+-adapted animals [26].

Arriving at this point, we thought it was crucial for the understanding of the cellular mechanisms of K^+ adaptation to analyze the conductance properties of the individual cell membranes and the paracellular shunt pathway in diluting segments of both control and K^+ adapted animals. Thus we applied cable analysis techniques on the amphibian diluting segment to investigate the specific cell membrane resistance at both conditions.

Materials and Methods

Amphiuma (obtained from C.C. Sullivan, Nashville, TE) were kept in glass tanks under two different conditions: One group of animals (control animals) was kept in regular tap water containing small amounts of salt (10 mmol · liter^{-1} NaCl, 0.3 mmol · liter^{-1} KCl). The other group (K^+-adapted animals) was kept in a 50 mmol · liter^{-1} KCl solution for about 5 weeks.

* *Permanent address:* Department of Physiology, University of Wurzburg, D-8700 Wurzburg, Federal Republic of Germany.

** *Permanent address:* Department of Physiology, The Johns Hopkins University School of Medicine, Baltimore, Maryland.

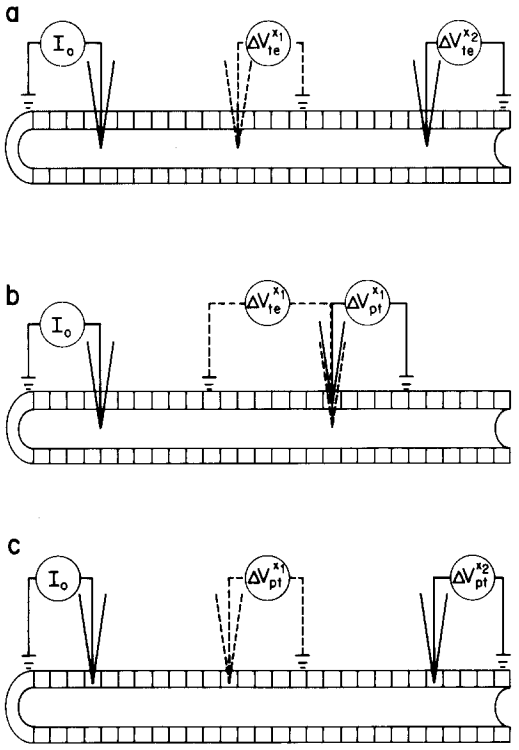

Fig. 1. Technique of cable analysis. (*a*) Luminal cable. A current delivering electrode (I_o) is inserted into the lumen. Another electrode, recording voltage changes (ΔV_{te}), is placed into the lumen at different distances (x) from the current electrode. (*b*) Measurement of voltage divider ratio (α). One electrode (I_o) delivers current pulses into the lumen, the other electrode (electrode tip in a cell) records voltage changes across the peritubular cell membrane and subsequently across the whole early distal epithelium (electrode tip in the lumen) at identical distance from the current electrode. (*c*) Cellular cable. The current electrode (I_o) is inserted into an early distal cell. Another voltage recording electrode (ΔV_{pt}) is placed into early distal cells at different distances (x)

Preparation of the kidney for double perfusion and perfusion methods have been described in detail previously [23]. The control perfusion solution had the following composition (mmol · liter^{-1}): NaCl 75, KCl 3, $CaCl_2$ 1.8, $MgCl_2$ 1, Na_2HPO_4 0.56, NaH_2PO_4 0.14, $NaHCO_3$ 20, glucose 5.5, glycine 3.3, polyvinylpyrrolidone 0.4. The lumen of the tubule under study was perfused via single-barreled micropipettes (tip diameter 12 μm), filled with control perfusion solution without glucose, glycine and polyvinylpyrrolidone. For estimation of the luminal K^+ conductance perfusion solutions with K^+ concentrations of 3 mmol/liter and 1 mmol/liter (Na^+ substituted for K^+) were used. Double-barreled micropipettes were used for rapid solution changes in the luminal compartment while the peritubular perfusate (with the same K^+ concentration) was exchanged simultaneously in the peritubular capillaries. All perfusion solutions were equilibrated with 1%, CO_2, 99% O_2 (pH 8.0). Since it is known that the electrical properties of the amphibian distal tubule change along this segment, tubules were selected with V_{te}-values of at least 5 mV (lumen positive *vs.* ground). It was previously proposed that tubules with V_{te}-values of $\geq$5 mV can be safely considered as diluting segments [31].

Conventional microelectrodes were drawn on a micropipette puller (Model PD-5, Narishige Scientific Instruments, Tokyo, Japan) from 1.2 mm OD, 0.6 mm ID capillary tubing (Federick Haer, Brunswick, ME) and filled with 1 mol/liter KCl. Electrical potential differences were measured by means of an electrometer (Model KS 700, Channel A, W.P. Instruments, New Haven CT) and current pulses generated by a constant current source (Model KS 700, Channel B).

All electrode electrometer connections were made with Ag/AgCl half cells. Potential differences were measured with respect to a 3 mol/liter KCl agar bridge on the surface of the kidney connected to ground by a Ag/AgCl half cell. Peritubular cell membrane potential (V_{pt}) and transepithelial potential difference (V_{te}) were measured by means of intracellular and intraluminal impalements with conventional microelectrodes. The luminal cell membrane potential difference (V_{lu}) was calculated from

$$V_{lu} = V_{te} - V_{pt}. \quad (1)$$

Resistance Measurements

The specific resistance of the luminal cell membrane (R_{lu}), the peritubular cell membrane (R_{pt}) and the paracellular shunt (R_s) were obtained from measurements of the transepithelial resistance (R_{te}), the resistance of both cell membranes in parallel (R_z), and the ratio of luminal to peritubular cell membrane resistance R_{lu}/R_{pt}. This method assumes that the epithelium can be modeled by a simple equivalent circuit in which all resistances are lumped into three components, the luminal cell membrane resistance (R_{lu}), the peritubular cell membrane resistance (R_{pt}) and the paracellular shunt resistance (R_s).

The experimental set-up used to measure the transepithelial resistance is illustrated in Fig. 1*a*. A current-passing microelectrode was inserted into the lumen of a diluting segment. Current pulses ranging from 10^{-8} to 10^{-7} A were passed through the current microelectrode by means of a constant current source. While the current electrode remained in place, several luminal impalements were made at different distances by a second microelectrode to record the voltage defections resulting from current injection into the lumen. The distance between current electrode and potential-recording electrode was measured with an ocular micrometer. From these measurements the length constant λ_{lu} and R_{te} can be determined as described in detail previously [2, 3, 6, 13].

The resistance in parallel of the luminal and peritubular cell membrane was estimated using a two-dimensional model similar to the technique used in sheet epithelia [6, 28] but adjusted for the special geometry of the renal tubule [2, 13, 35, 36]. As shown in Fig. 1*c*, depolarizing current pulses ranging from 1×10^{-8} to 5×10^{-7} A were injected into a cell by means of an intracellular microelectrode. Changes of the basolateral cell membrane potential, resulting from current pulses were measured by means of a series of cell impalements with a second microelectrode. These measurements allow the evaluation of the length constant of the cell cable λ_c and of the cell cable specific resistance ζ_c [13].

The voltage-divider ratio α ($\Delta V_{te}/\Delta V_{pt} - 1$) was evaluated as follows (Fig. 1*b*): Current pulses 5×10^{-8} and 5×10^{-7} A, 1 sec duration, were injected into the lumen via one microelectrode while another electrode was advanced sequentially into a cell across the peritubular membrane and into the lumen across the luminal cell membrane.

The absolute values of R_z, R_{lu}, R_{pt}, and R_s (paracellular

shunt resistance) were calculated according to equations described previously [13].

Experimental Procedures for Evaluating the Potassium Conductance of the Luminal Cell Membrane

The cell membranes and the paracellular shunt can be modeled by electromotive forces in series with resistors. The electromotive forces correspond to the potentials (E_{lu}, E_{pt}, E_s), which would be measured across a given membrane or the shunt if no current were flowing in the circuit.

The K^+ conductance of the luminal (G^K_{lu}) cell membrane is defined as

$$G^K_{lu} = G_{lu} \cdot t^K_{lu} \tag{2}$$

where G_{lu} is the total conductance of the luminal cell membrane, $1/R_{lu}$, and t^K_{lu} the K^+ transference number which was determined by the following technique: Peritubular and luminal compartments of a diluting segment were perfused with solutions containing 3.0 mmol/liter K^+. Changes in V_{te} and V_{pt} were recorded after both luminal *and* peritubular solutions were switched *simultaneously* to a solution containing 1 mmol/liter K^+. The change in the electromotive force of the luminal cell membrane (ΔE_{lu}), induced by the K^+ concentration step change can be calculated from

$$\Delta E_{lu} = \Delta V_{lu} + \Delta V_{te} \frac{R_{lu}}{R_s}. \tag{3}$$

This approach assumes that small, symmetrical changes in the concentration of K^+ in both luminal and peritubular perfusion solutions do not change the resistances of the cell membranes and of the shunt significantly and that ΔE_s remains zero. Since per definition the cell membrane conductance for a particular ion depends on its concentration, reduction of luminal K^+ concentration from 3 to 1 mmol/liter is expected to alter (i.e., reduce) the luminal K^+ conductance. This phenomenon has been observed in rat distal tubule even for small concentration changes [14]. However, in contrast to this study, the luminal cell membrane in our preparation appears to be K^+-selective, which minimizes this experimental problem. Therefore, E_{lu} was used to calculate t^K_{lu} by the following equation

$$t^K_{lu} = \frac{\Delta E_{lu}}{\frac{RT}{zF} \ln \frac{c^K_1}{c^K_3}} \tag{4}$$

where c^K_1 and c^K_3 are 1 and 3 mmol/liter K^+ concentrations of the perfusion solutions, respectively.

Statistics

In this study we did not measure R_{te}, R_z and R_{lu}/R_{pt} in the same tubule in order to avoid artefacts resulting from the multiple impalements required. We thus avoided a technical problem but added some statistical uncertainty. Because the measurements were done in separate tubules we can only use the mean values to calculate the individual resistances of the epithelium. As discussed previously [17], this prevents us from giving SEM and doing tests of significance on R_{pt}, R_{lu}, R_s, t^K_{lu} and G^K_{lu} in the two groups of animals. We assume that the values serve as reasonable approximations.

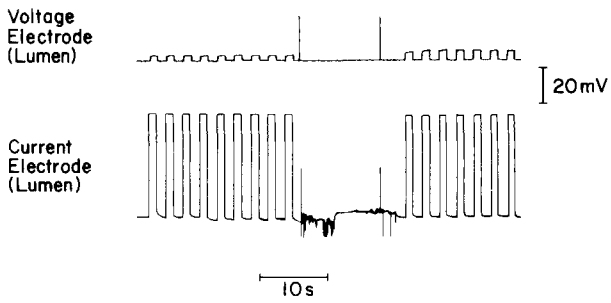

Fig. 2. Original recording of transepithelial resistance measurements (R_{te}) according to Fig. 1*a*. Lower tracing shows the current pulses of the intraluminal *current* electrode (voltage deflections are off scale in the tracing); the upper tracing reflects the induced voltage changes of the intraluminal *voltage* recording electrode obtained at two different distances from the current electrode

Some results of the study are reported as mean values ± SEM. Student *t*-test was used for comparison of means in the two groups of animals. Regression lines were calculated by the least squares method.

Results

Specific Transepithelial Resistance

Illustrated in Fig. 2 are two simultaneous tracings of voltage deflections detected by two microelectrodes which were placed in the lumen of an early distal tubule. The lower tracing is a recording from the current electrode, which was maintained in the same position throughout the experiment. The upper tracing is a recording from a second microelectrode, which was alternately placed in the tubular lumen at two locations from the current electrodes. The upward deflections in both tracings are the result of the injection of current pulses into the lumen from the current electrode. Figure 3 shows a logarithmic plot of ΔV_{te} versus distance for all tubules studied from both control and potassium adapted animals. The mean values of λ_{lu} and R_{te} calculated from the data presented in Fig. 3 are given in Table 1. As also evident from this table, adapting the animals to high K^+ medium decreases R_{te} significantly.

Specific Resistance of the Cell Membranes

A representative example of cell cable measurements is shown in Fig. 4. The lower tracings represent voltage deflections recorded by the current

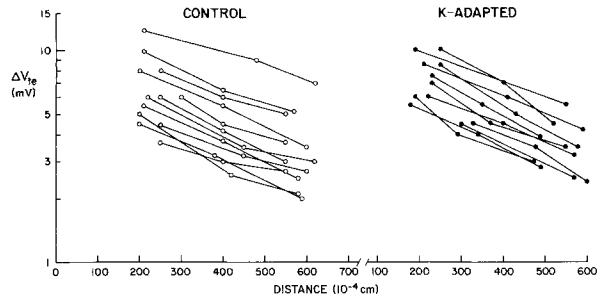

Fig. 3. Transepithelial voltage attenuation according to Fig. 1*a*. Open circles represent controls; closed circles represent experiments in the K^+-adapted animals. The lines join voltage deflections across the epithelium (ΔV_{te}) obtained in the same tubule at different distances. The slope is an expression of the length constant of the luminal cable (λ_{lu}); mean values are given in Table 1

Table 1. Lumen cable properties

	Control	K^+ adaptation
$\lambda_{lu}(10^{-4}$ cm)	567 ± 34	459 ± 18
$R_{te}(\Omega$ cm^2)	290 ± 27	199 ± 17[a]
$a(10^{-4}$ cm)	24 ± 1	23 ± 1
n	12	11

[a] $P < 0.05$, a = tubule inner radius.

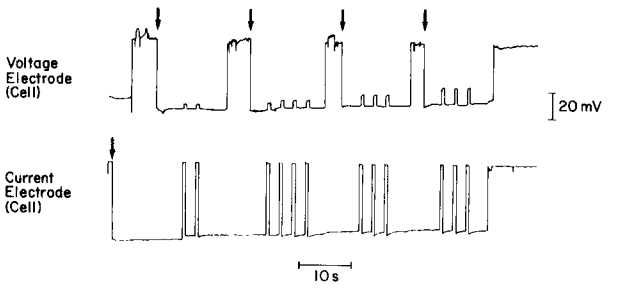

Fig. 4. Recording of the intraepithelial current spread (*see also* Fig. 1*c*). The lower tracing indicates the intracellular current application (voltage deflections are off scale); the upper recording shows the voltage deflections sensed by a voltage recording electrode placed intracellularly at different distances from the current electrode. While the current electrode remained in the same cell (lower trace) four different intracellular impalements were made with the other electrode at decreasing distance (upper trace, left to right) from the current electrode. The arrows mark the intracellular inpalements

electrode located in an early distal tubule cell. The voltage deflections are measured by a second microelectrode in several cells at various distances from the current electrode along the same tubule (upper tracing). The data for all tubules studied are plotted in Fig. 5, and the average values for ζ_c, λ_c,

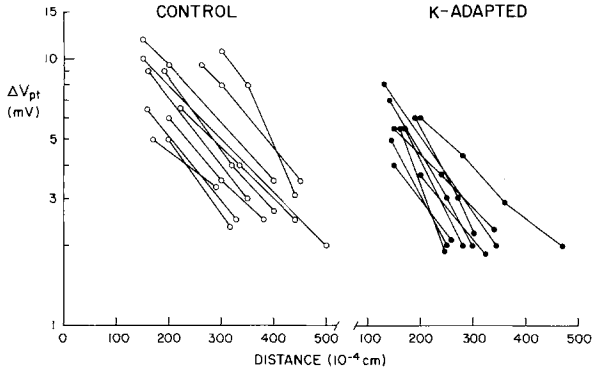

Fig. 5. Intraepithelial voltage attenuation according to Fig. 1*c*. The lines connect circles (open circles = control, closed circles = K^+ adapted), which indicate intracellularly measured voltage deflections (ΔV_{pt}) at various distances from an intracellular current source. Their slopes express the length constant of the cellular cable (λ_c); mean values are given in Table 2

Table 2. Cell cable properties and resistance ratio

	Control	K^+ adaptation
$\lambda_c(10^{-4}$ cm)	201 ± 12	151 ± 19[a]
$\zeta_c(\Omega$cm)	342 ± 43	545 ± 80
$R_z(\Omega$cm^2)	157 ± 14	108 ± 6[b]
$a(10^{-4}$ cm)	23 ± 2	22 ± 2
$d(10^{-4}$ cm)	8.2 ± 0.2	8.2 ± 0.2
n	10	10
$R_{lu}/R_{pt}(\alpha)$	2.5 ± 0.1	1.9 ± 0.1[b]
n	19	17

[a] $P < 0.05$;
[b] $P < 0.01$; a = tubule inner radius; d = thickness of the cell layer.

and R_z are given in Table 2. Importantly, both λ_c and R_z are significantly lower in K^+-adapted kidneys in comparison to control.

Resistance Ratio of Luminal to Peritubular Cell Membranes

Figure 6 represents measurements of the voltage-divider ratio of luminal to peritubular cell membranes in control and K^+-adapted animals. The voltage-divider ratio was used as an estimate of the resistance ratio. The data are summarized in Table 2. The ratio of R_{lu} to R_{pt} is significantly lower in early distal cells of K-adapted kidneys than in control kidneys.

Luminal and Peritubular Cell Membrane and Paracellular Shunt Resistance

From R_{te}, R_z and R_{lu}/R_{pt} the individual cell membrane and paracellular shunt resistances were cal-

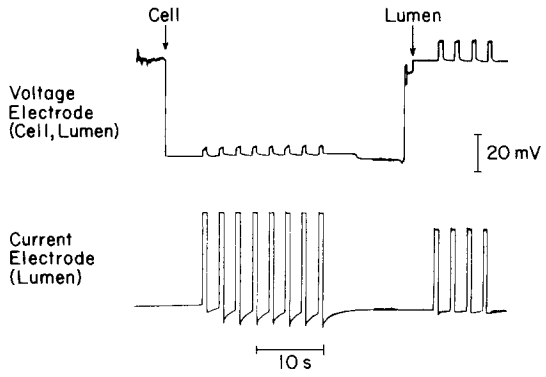

Fig. 6. Measurement of the resistance ratio (R_{lu}/R_{pt}) according to Fig. 1*b*. The lower tracing indicates intraluminal current injection (voltage deflections are off scale); the upper tracing demonstrates the voltage change across the peritubular membrane (electrode intracellularly) and subsequently across the whole epithelium (electrode intraluminally) at identical distance from the intraluminal current electrode. The mean values of R_{lu}/R_{pt} are displayed in Table 2

Table 3. Estimates of cellular and paracellular resistances

	Control	K^+ adaptation
$R_{pt}(\Omega cm^2)$	219	162
$R_{lu}(\Omega cm^2)$	550	324
$R_s(\Omega cm^2)$	306	336

culated according to equations published previously [13]. The data are summarized in Table 3. In control animals the combined resistance of the transcellular pathway ($R_{lu} + R_{pt}$) is 769 Ωcm^2. It is only about 2.5 × the resistance of the paracellular pathway, indicating that the conductance of the transcellular and paracellular pathways are in the same order of magnitude. Similar conclusions were derived from recent experiments in the cortical thick ascending limb of rabbit kidney [9]. This situation is different from the proximal tubule where the major conductive pathway is the paracellular shunt pathway. In *Necturus* proximal tubule the ratio of transcellular resistance to shunt resistance is about 29 [13] and about 200 in the rat proximal tubule [7].

Adaptation to high potassium results in a decrease in the individual cell membrane resistances (Table 3). Perhaps the most striking decrease occurs at the luminal cell membrane where R_{lu} is reduced by some 40%.

Potassium Transference Number and Conductance of the Luminal Cell Membrane

Transepithelial potential, luminal and peritubular cell membrane potential differences are given in Table 4. There is a slight but significant increase of V_{pt} found after K^+ adaptation which explains the significant reduction of V_{te}. These values are not different from those reported previously [21].

Table 4. Cell membrane and transepithial potential differences

	Control	K^+ adaptation
V_{pt}(mV)	−72.6 ± 0.2	−75.1 ± 0.7[a]
V_{lu}(mV)	80.7 ± 0.7	81.3 ± 0.9
V_{te}(mV)	8.2 ± 0.4	6.2 ± 0.3[a]
n	19	17

[a] $P < 0.05$.

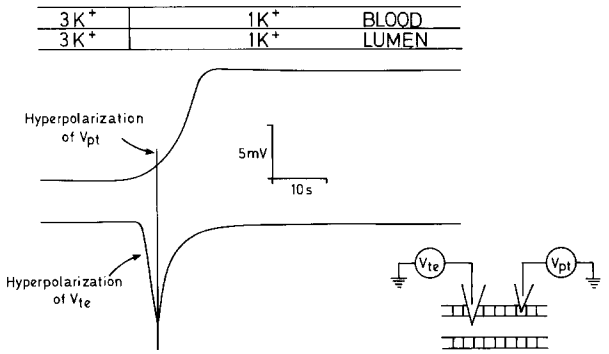

Fig. 7. Drawings from original recordings. The transepithelial and the peritubular cell membrane potential differences (V_{te}, V_{pt}) were recorded by microelectrodes located in lumen and cell, respectively. Peritubular and luminal perfusates were simultaneously switched from 3 to 1 mmol/liter KCl. ΔV_{te} and ΔV_{pt} values were taken for further calculations at the points where the vertical line cuts the recordings. Hyperpolarization of V_{pt} = cell interior becomes more negative. Hyperpolarization of V_{te} = lumen becomes more positive

Table 5. Estimation of luminal transference numbers and K^+ conductances from simultaneous K^+ concentration step-changes (3 *vs.* 1 mmol/liter) on both cell membranes

	Control	K^+ adaptation
ΔV_{te}(mV)	11.2 ± 1.1	14.7 ± 0.8[a]
ΔV_{pt}(mV)	3.3 ± 0.9	3.8 ± 0.8
ΔV_{lu}(mV)	14.3 ± 1.2	18.8 ± 0.6[a]
ΔE_{lu}(mV)	34.4	33.0
t^k_{lu}	1.22	1.17
G^k_{lu}(mS cm^{-2})	2.2	3.6
n	10	9

[a] $P < 0.05$

When the peritubular and the lumen K^+ is simultaneously changed from 3 to 1 mmol/liter and vice versa, *transient* changes of the transepithelial and the cell membrane potentials can be observed (Fig. 7 and Table 5). For instance, when the perfusate is switched from a K^+ concentration of 3 to 1

mmol/liter, V_{te} hyperpolarizes (the lumen becomes more positive). However, V_{te} relaxes after some seconds and returns back to about the initial value. The peritubular cell membrane potential increases only a few mV in the first phase but continues to hyperpolarize gradually in the second phase. Values were taken from the first phase of the hyperpolization (peak values of ΔV_{te}, Table 5) since the second phase of the potential response occurred gradually and appeared due to changes of intracellular ion composition and/or changes of cell membrane conductance.

According to Eq. (3), the induced changes of the electromotive forces of the lumen cell membrane can be estimated for both groups of animals. From the data in Tables 3 and 5 and using Eq. (4), the potassium transference number and the potassium conductance of the luminal cell membrane can be estimated. They are also given in Table 5. Theoretically, the transference number of a particular ion could at best approach unity but not at all exceed it. If in this preparation corrections for cable-to-cable interactions are applied (*see* Appendix) and the corrected resistance values are used in Eq. (3), then t_{lu}^{K} values for control and K^+-adapted animals of 0.83, and 0.99, respectively, are calculated. The data indicate that in both groups of animals the lumen cell membrane is K^+ selective and that the absolute potassium conductance increased by some 60% in K^+ adaptation. This dramatic increase in absolute potassium conductance, combined with the increase in intracellular K^+, which occurs during K^+ adaptation [23], are major factors involved in reversing the direction of K^+ net transport from reabsorption to secretion after K^+ adaptation.

Discussion

Critique of the Methods

It is known from recent experiments in mammalian [9] and amphibian tubules [1, 13] that analyzing the spatial decay of voltage in lumen and cell cable is not without pitfalls because of possible cable-to-cable interactions or "crosstalk." Therefore, special care was taken to reduce the influence of "crosstalk" on the obtained resistance values. As demonstrated in the mammalian cortical thick ascending limb of Henle's loop [10] some length dependence of the apparent cell membrane resistance ratio has been observed resembling "crosstalk" as also discussed recently for the amphibian proximal tubule [1, 13, 16]. Furthermore, it is known that the evaluation of the length constant of the cell cable at distances of more than 700 μm from the current source may cause a significant error [1, 13] either due to significant cable-to-cable interaction (especially when $\lambda_{lu} \gg \lambda_c$ and when the transcellular resistance approaches the paracellular shunt resistance) and/or due to the fact that at such long distances the amplitude of the induced voltage deflections for current strengths, applied in this study, become too small to be measured experimentally. On the other hand, evaluation of the length constant of the cell cable at distances shorter than 250 μm from the current source may also falsify the results [13]. Finally, the length dependence of the cell membrane resistance ratio appears to be enlarged at short distances as shown in the mammalian isolated tubule [10].

Consequently, we recorded induced electrotonic voltage deflections only at distances between about 200 and 600 μm from the current source. We tried to avoid extreme current densities that may affect intracellular ion composition and/or change the resistance properties of the cell membrane. Finally, we estimated the influence of "cross-talk" in a carbon-resistor model, explained in detail in the appendix of this paper.

Luminal K^+ Conductance and Resistance Measurements

The K^+ transference number of the luminal cell membrane is close to unity, which supports previous findings that the lumen cell membrane is K^+ selective [22]. Then, the electromotive force of this individual cell barrier (E_{lu}) can be calculated according to the equation

$$E_{lu} = V_{lu} + V_{te} \frac{R_{lu}}{R_s}. \tag{5}$$

Assuming a K^+-selective luminal cell membrane, E_{lu} and extracellular K^+ are used to estimate intracellular potassium. An intracellular K^+ activity of about 70 mmol · liter^{-1} is calculated assuming that K^+ is the only diffusible ion of the luminal cell membrane and no electrogenic transport process is operative across this cell barrier. This value agrees well with previous ion-selective microelectrode measurements in early distal cells of the amphibian kidney [21] and the mammalian thick ascending limb [9].

The present data demonstrate that the transcellular resistance ($R_{lu} + R_{pt}$) is of about the same order of magnitude as compared with the paracellular shunt resistance. Therefore, the measured cell membrane potentials approach the respective electromotive forces even in the presence of a signifi-

cant transepithelial potential difference. This quantitative relationship between the magnitude of cell membrane resistance and paracellular shunt resistance is documented by the previous observation that in diluting segments of the doubly-perfused *Amphiuma* kidney furosemide *does not* change V_{lu} considerably while the lumen positive V_{te} is completely abolished [19]. Applying Eq. (3) it becomes obvious that the resistance ratio R_{lu}/R_s determines the furosemide-induced ΔV_{lu}. Since this ratio is small in our preparation, altering V_{te} will have only moderate influence on V_{lu}. However, in the *isolated* amphibian diluting segment lower R_{te} values have been reported [29] and thus, lower R_s-values are likely in this preparation. This allows a significant circular current at control conditions (i.e., in the presence of a lumen positive potential difference) which depolarizes V_{lu} considerably. Then, elimination of circular current (by application of furosemide) hyperpolarizes V_{lu} considerably.

Studies in the distal tubule of triturus kidney [31] give significantly lower estimates of R_{te} as compared to our study, performed in the same nephron segment. The authors of the former study assumed that in their *in vivo* preparation luminal NaCl-concentration was similar to the extracellular one (85 mmol/liter). Recent experiments, however, indicate that the tubule fluid is progressively diluted downstream [32] and luminal Cl^- can be as low as 20 mmol/liter [24]. Therefore, the luminal fluid resistivity is increased about four times and consequently four times higher R_{te} values are calculated, which then agree well with our reported R_{te} values.

Potassium Adaptation

Mammals chronically exposed to a high K^+ diet adapt by increasing dramatically the ability of the late distal portions of the kidney to secrete K^+ (reviewed in [8]). Amphibians can also adapt to exposure to high K^+ in their environment by a similar mechanism, however, in contrast to the mammalian kidney, the increase of K^+ secretion occurs in the early distal tubule [20, 34] at the level of the diluting segment. One explanation for an increased net K^+ secretion as shown in this study is that the absolute luminal K^+ conductance is increased dramatically by K^+ adaptation. The increased K^+ conductance allows an increased transport of K^+ from the cell into the lumen. Although there is no doubt that the increased conductance plays an important role in increasing K^+ secretion, it is not the only factor involved.

For example, in the mammalian kidney, chronically increased K^+ intake acts to enhance Na^+/K^+ pump activity in the last distal nephron [5, 30]. In the *Amphiuma* kidney, a chronic increase in K^+ leads to an increase in intracellular K^+ activity of early distal tubule cells [21]. Thus the increased pump activity, leading to an increase of intracellular K^+ together with a larger luminal K^+ conductance could be important factors in enhancing K^+ secretion in the distal nephron.

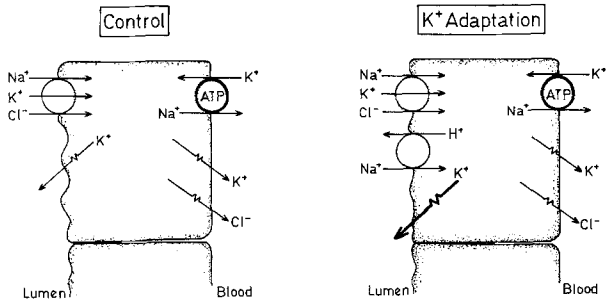

Fig. 8. Cell model of the amphibian diluting segment

In addition to its effects on the luminal K^+ conductance, K^+ adaptation also influences the luminal $Na^+/K^+/Cl^-$ cotransport system. In control animals, the early distal tubule normally reabsorbs a small amount of potassium. The reabsorption of K^+ is indicative of a small imbalance between the influx of K^+ via the cotransport system and the conductive pathway. The diuretic furosemide, by inhibiting the luminal cotransport system, induces net K^+ secretion in control kidneys but does not further enhance K^+ secretion in K^+-adapted animals [20]. This suggests that transport by the luminal contransport system may be reduced by K^+ adaptation. This is supported by the observation that the magnitude of the transepithelial potential difference which correlates well with Cl^- transport in this segment as well as the electrochemical potential difference of Cl^- across the epithelium are decreased after K^+ adaptation [24]. Both of these observations, in suggesting that net chloride reabsorption is diminished by K^+ adaptation, point to an inhibition of the luminal contransporter.

The present data suggest that the increase of the absolute luminal K^+ conductance is a major characteristic of K^+ adaptation. Based on recent observations we like to offer a hypothesis on the underlying mechanism (Fig. 8): Studies in the amphibian diluting segment indicate that the luminal K^+ conductance is highly pH-sensitive [12, 18]. Furthermore, a luminal Na^+/H^+ exchange system is activated after K^+ adaptation [23]. The direct stimulus for the activation of the Na^+/H^+ exchanger is most likely the corticosteroid hormone aldosterone, which is found in excessive concentrations in the plasma of

K^+-adapted amphibians [26] and which does stimulate the Na^+/H^+ exchange in this tubule segment [33]. Therefore, it is tempting to postulate that in K^+ adaptation the primary event is the aldosterone-induced activation of the luminal Na^+/H^+ exchange system, which in turn increases the luminal K^+ conductance via an increase of intracellular pH.

This work was supported by Deutsche Forschungsgemeinschaft SFB 176 (46) and by U.S. Public Health Service Grant AM 174 33. We thank Drs. F. Lang and R. Greger for their constructive criticism during the course of the study. We are grateful to Mrs. Derrick and Mrs. Ramoz for their excellent and patient secretarial assistance.

References

1. Anagnostopoulos, T., Toulon, J., Edelman, A. 1979. Conductance properties of the proximal tubule in *Necturus* kidney. *J. Gen. Physiol.* **75:**553–587
2. Anagnostopoulos. T., Velu, T. 1974. Electrical resistance of cell membranes in *Necturus* kidney. *Pfluegers Arch.* **346:**327–339
3. Boulpaep, E.L., Giebisch, G. 1978. Electrophysiological measurements on the renal tubule. *In:* Methods in Pharmacology. Vol. *4*B, pp. 165–193. Manuel Martinez-Maldonado, editor. Plenum, New York
4. Burg, M.B., Green, N. 1973. Function of the thick ascending limb of Henle's loop. *Am. J. Physiol.* **224:**659–668
5. Finkelstein, F.O., Hayslett, J.P. 1975. Role of medullary Na-K-ATP-ase in renal potassium adaptation. *Am. J. Physiol.* **229:**524–528
6. Frömter, E. 1972. The route of passive ion movement through the epithelium of *Necturus* gallbladder. *J. Membrane Biol.* **8:**259–301
7. Frömter, E. 1977. Magnitude and significance of the paracellular shunt pathway in rat kidney proximal tubule. *In:* Intestinal Permeation. M. Kramer and F. Lauterbach, editors. Exeptor Medica, Amsterdam
8. Giebisch. G. 1979. Renal potassium transport. *In:* Transport Across Biological Membranes. G. Giebisch, D. Tosteson, and H.H. Ussing, editors. Springer Verlag, Berlin
9. Greger, R. 1985. Ion transport mechanism in the thick ascending limb of Henle's loop of the mammalian nephron. *Physiol. Rev.* **65:**761–797
10. Greger, R., Schlatter, E. 1982. Properties of the lumen membrane of the cortical thick ascending limb of Henle's loop of rabbit kidney. *Pfluegers Arch.* **396:**315–324
11. Guggino, W.B., Oberleithner, H., Giebisch, G. 1985. Relationship between cell volume and ion transport in the early distal tubule and the *Amphiuma* kidney. *J. Gen. Physiol.* **86:**31–58
12. Guggino, W.B., Stanton, B.A., Giebisch, G. 1982. Regulation of apical potassium conductance in the isolated early distal tubule of the *Amphiuma* kidney. *Biophys. J.* **37:**338 (*abstr.*)
13. Guggino, W.B., Windhager, E.E., Boulpaep, E.L. Giebisch. G. 1982. Cellular and paracellular resistances of the *Necturus* proximal tubule. *J. Membrane Biol.* **67:**143–154
14. Hayslett, J.P., Boulpaep, E.L., Giebisch, G.H. 1978. Factors influencing transepithelial potential difference in mammalian distale tubule. *Am. J. Physiol.* **234:***F*182–*F*191
15. Hebert, S.C., Friedman, P.A., Andreoli, T.E. 1984. Effects of antidiuretic hormone on cellular conductive pathways in mouse thick ascending limbs of Henle: I. ADH increases transcellular conductance pathways. *J. Membrane Biol.* **80:**201–219
16. Hoshi, T., Kawahara, K., Yokoyama, R., Suenaga, K. 1980. Changes in membrane resistance of renal proximal tubule induced by contransport of sodium and organic solute. *Union Physiol. Sci.* **14:**479 (*abstr.*)
17. Matsumura, Y., Cohen, B., Guggino, W.B., Giebisch, G. 1984. Regulation of the basolateral potassium conductance of the *Necturus* proximal tubule. *J. Membrane Biol.* **79:**153–161
18. Oberleithner, H., Dietl, P., Munich, G., Weigt, M., Schwab, A. 1985. Relationship between luminal Na^+/H^+ exchange and luminal K^+ conductance in diluting segment of frog kidney. *Pfluegers Arch.* (*in press*)
19. Oberleithner, H., Guggino, W., Giebisch, G. 1982. Mechanism of distal tubular chloride transport in *Amphiuma* kidney. *Am. J. Physiol.* **242:***F*331–F339
20. Oberleithner, H., Guggino, W., Giebisch, G. 1982. The effect of furosemide on luminal sodium, chloride and potassium cotransport in the early distal tubule of *Amphiuma* kidney. *Pfluegers Arch.* **396:**27–33
21. Oberleithner, H., Guggino, W., Giebisch, G. 1983. Potassium transport in the early distal tubule of *Amphiuma* kidney. *Pfluegers Arch.* **396:**185–191
22. Oberleithner, H., Lang, F., Greger, R., Wang, W., Giebisch, G. 1982. Effects of luminal potassium on cellular sodium activity in early distal tubule of *Amphiuma* kidney. *Pfluegers Arch.* **396:**34–40
23. Oberleithner, H., Lang, F., Messner, G., Wang, W. 1984. Mechanism of hydrogen ion transport in the diluting segment of frog kidney. *Pfluegers Arch.* **402:**272–280
24. Oberleithner, H., Lang, F., Wang, W., Deetjen, P. 1982. Potassium (K^+)-adaptation affects chloride (Cl^-) reabsorption in the diluting segment of *Amphiuma*. *Nieren- und Hochdruckkrankheiten* **5:**180
25. Oberleithner, H., Lang, F., Wang, W., Giebisch, G. 1982. Effects of inhibition of chloride transport on intracellular sodium activity in distal amphibian nephron. *Pfluegers Arch.* **394:**55–60
26. Oberleithner, H., Lang, F., Wang, W., Messner, G., Deetjen, P. 1983. Evidence for an amiloride sensitive Na^+ pathway in the amphibian diluting segment induced by K^+ adaptation. *Pfluegers Ach* **399:**166–172
27. Oberleithner, H., Ritter, M., Lang, F., Guggino, W. 1983. Anthracene-9-carboxylic acid inhibits renal chloride reabsorption. *Pfluegers Arch.* **398:**172–174
28. Reuss, L., Finn, A.L. 1975. Electrical properties of the cellular transepithelial pathway in *Necturus* gallbladder: I. Circuit analysis and steady-state effects of mucosal solution ionic substitution. *J. Membrane Biol.* **25:**115–139
29. Sackin, H., Morgunov, N., Boulpaep, E.L. 1982. Electrical potentials and luminal membrane ion transport in the amphibian diluting segment. *Fed. Proc.* **41:**1495 (*abstr.*)
30. Silva, P., Brown, R.S., Epstein, F.H. 1974. Adaptation to potassium. *Kidney Int.* **11:**466–475
31. Teulon, I., Anagnostopoulos, T. 1982. The electrical profile of the distal tubule in triturus kidney. *Pfluegers Arch.* **395:**138–144
32. Teulon, I., Froissant, P., Anagnostopoulous, T., 1985. Elec-

trochemical profile of K^+ and Na^+ in the amphibian early distal tubule. *Am. J. Physiol.* **248:**F266–F271
33. Weigt, M., Schwab, A., Oberleithner, H. 1985. Aldosterone acutely stimulates amiloride-sensitive H^+ net secretion in diluting segment of frog kidney. *Pfluegers Arch.* **Suppl. 403:***R*15
34. Wiederholt, M. Sullivan, W.J., Giebisch, G. 1971. Potassium and sodium transport across single distal tubules of *Amphiuma*. *J. Gen. Physiol.* **57:**495–525
35. Windhager, E.E., Boulpaep, E.L., Giebisch, G. 1966. Electrophysiological studies on single nephrons. Third International Congress of Nephrology. Vol. 1, pp. 35–47
36. Windhager, E.E., Giebisch, G. 1965. Electrophysiology of the nephron. *Physiol. Rev.* **45:**214

Received 12 February 1985; revised 26 July 1985

Appendix

In order to estimate the possible magnitude of cable-to-cable interactions in the early distal tubule, a resistor model of the tubule was built according to the electrical circuit model published previously [13]. Resistance values were chosen such that the resistances approximated (per length of tubule) those measured in the diluting segment. Ten elements were connected together, each representing 100 μm length of tubule. At either end of the 100-μm element series an element representing 1000 μm length of tubules was placed. These 1000-μm elements were used to increase the length of the model in order to mimic an infinite cable model. 100 nA of current was injected either into the *luminal* cable or the *cellular* cable between the 1000-μm element and the first 100-μm element. Figure 9 (left panel) shows a semilog-plot of the electrotonic voltages resulting from current injection into the *luminal* elements. The upper trace depicts the electrotonic voltages measured across the luminal elements at various distances. The length constant of the luminal cable of the model is 626 μm, a value similar to λ_{lu} reported in Table 1.

Electronic voltages measured in the cellular elements are shown in the middle trace of Fig. 9 (left panel), and the calculated voltage-divider ratios are shown in the lower trace. As discussed previously [13], the voltage-divider ratio is a function of distance only at distances near to the current source. At distances beyond 300 μm the voltage-divider ratio becomes independent of distance.

Plotted as a function of distance in Fig. 9 (right panel) are the electronic voltages resulting from injection of current into the *cellular* elements. It is interesting to note that beyond about 350 μm from the intracellular current source, the electrotonic voltage deflections in the luminal elements are larger than those in the cellular elements. This crossover indicates cable-to-cable interactions. The presence of the luminal cable influences the properties of the cellular cable. Since λ_{lu} is greater than λ_c, the measured λ_c will be greater than the true value. The length constant, calculated from a fit of the data to a single exponential is 243 μm, a value similar to the one reported in Table 2 for the cell cable. However, as shown in Fig. 9, the calculated length constant increases with distance from the current electrode. In order to verify that the dependence on distance is caused to cable-to-cable interactions, the luminal elements were grounded to eliminate cross talk between the cables. Under these circumstances, the electrotonic voltage decay behaved as one exponential with a length constant of 183 μm. Thus, it is clear that cable-to-cable interactions occur in our model and lead to an overestimate of the cellular length constant.

The magnitude of the error introduced by cable-to-cable interactions can be assessed further by calculating R_z from the data obtained both *with* and *without* (grounded luminal elements) cable interactions. In the unaltered model the calculated R_z is 265 Ω cm^2 and, as expected, the calculated R_z after correction for "cross talk" is lower, at 221 Ω cm^2. Although the cable interactions do influence the measurement of R_z, it is obvious that in this case the influence is not large.

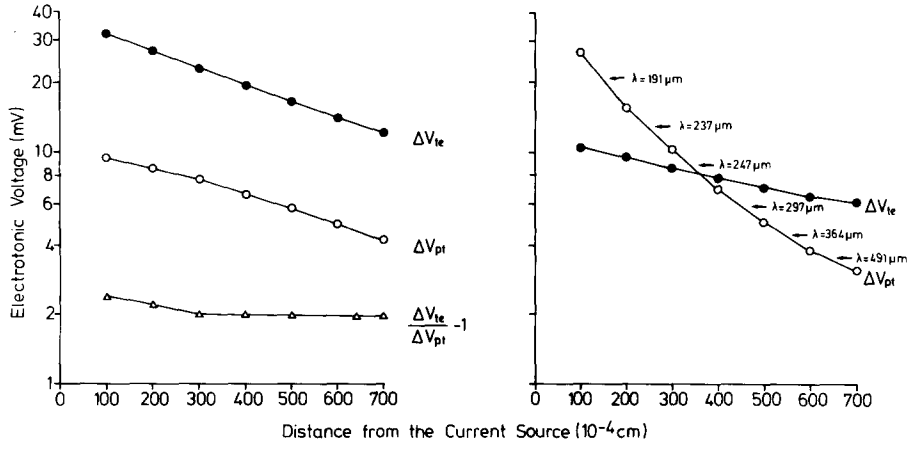

Fig. 9. Data obtained from the resistor model which mimics the resistance properties of the amphibian diluting segment. Left: Current (10^{-7} A) was injected into the luminal cable. The current-induced voltage deviations are plotted *vs.* distance from the current source. Right: Current injected into the cellular cable